

Nonaqueous MEA/PEG200 Absorbent with High Efficiency and Low Energy Consumption for CO₂ Capture

Wen Tian, Kui Ma, Junyi Ji, Siyang Tang, Shan Zhong, Changjun Liu, Hairong Yue, and Bin Liang*



Cite This: *Ind. Eng. Chem. Res.* 2021, 60, 3871–3880



Read Online

ACCESS |

Metrics & More

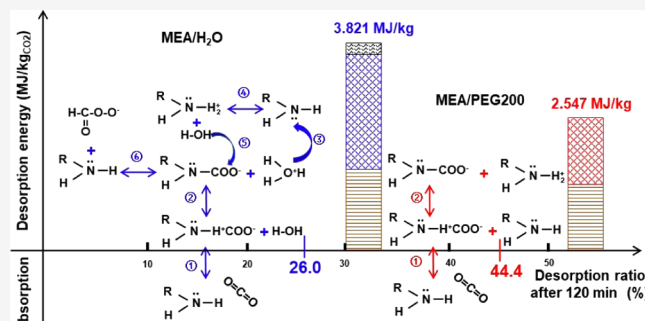
Article Recommendations

Supporting Information

ABSTRACT: CO₂ capture by stripping with aqueous amine is a well-understood and widely employed technology. However, there still exist several drawbacks in the practical applications, such as high energy consumption and serious equipment corrosion. In this paper, an organic monoethanolamine/poly(ethylene glycol) 200 (MEA/PEG200) absorbent with low specific heat capacity, low vapor pressure, and a high boiling point was developed to substitute the aqueous amine systems. The absorption rate and capacity, the desorption rate, and regeneration efficiency, as well as the thermal stability of the absorbent were systematically investigated. For instance, the 3 M MEA/PEG200 absorbent exhibited the highest desorption rate (838 mg_{CO₂}/(L_{sol}·min)) and excellent cyclic stability (deviation < 4%), which was much superior to the 3 M MEA/H₂O absorbent (447 mg_{CO₂}/(L_{sol}·min)). In addition, the desorption energy consumption of the MEA/PEG200 absorbent was 33% lower than that of the MEA/H₂O. Moreover, both fresh and CO₂-rich MEA/PEG200 solutions exhibited only slight corrosion to carbon steels even after being immersed for 400 days. Therefore, this low-energy-consuming and anticorrosive MEA/PEG200 absorbent reveals the potential for industrial CO₂ capture.

1. INTRODUCTION

Global annual energy-related CO₂ emissions rose to a historic high value of 33.1 Gt in 2018.¹ The excessive amount of CO₂ emission has a significant impact on agriculture, water resources, ecosystem, and human health. It is of great significance to promote the low-carbon technologies to reduce the CO₂ emissions. Particularly, the CO₂ capture, utilization, and storage (CCUS) is considered as one of the most effective methods to achieve CO₂ emission reduction.² Alkanolamine solvent absorption from the industrial flue gas is one of the dominant CO₂ capture technologies due to its high separation efficiency, good selectivity, and cycling stability. Meanwhile, the purity of CO₂ regenerated from an organic amine solvent is relatively high, which can be applied as a raw material to further produce the downstream products, such as carbonate, urea, organic chemicals, etc.^{3,4} Aqueous amines are a major solvent group for commercial absorption. However, they possess large specific heat capacity, high sensible heat and latent heat of vaporization, and high decomposition temperature (120–150 °C) in regeneration.⁵ The heat duty for solvent regeneration can constitute up to 70% of the total operating costs in a CO₂ capture plant.^{6–8} Meanwhile, the amine aqueous solution is also corrosive for the equipment.^{9,10} Therefore, developing various new solvents is crucial to improve the energy efficiency and operation safety during the CO₂ capture process.



The current research studies on a CO₂ capture solvent mainly focus on developing an absorbent with a high absorption rate, large capacity, low specific heat capacity, and low saturated vapor pressure. For example, ionic liquids possess large CO₂ absorption capacity, but the high cost and high viscosity hinder their industrial applications.^{11,12} Phase-change absorbents can automatically separate a CO₂-rich-phase from a poor-phase solution; the energy consumption can be reduced by cutting the amount of the absorbent loaded in a regenerator.^{13,14} However, phase changeable solvents are still expensive, and the CO₂-rich liquid phase generally possesses high viscosity, which is not conducive to desorption.¹⁵ Nonaqueous solutions, especially the organic alcohol solvents [e.g., triethylene glycol, propylene glycol, ethylene glycol, and poly(ethylene glycol) (PEG)], are considered as one class of the promising solvents. The polar hydroxyl groups on the organic alcohol solvents have higher affinity for CO₂ molecules, thereby improving the CO₂ capture capacity.^{16–18} On the other hand, the organic alcohols usually exhibit lower

Received: October 29, 2020

Revised: February 20, 2021

Accepted: February 23, 2021

Published: March 8, 2021



isobaric specific heat capacity compared with that of the water, which can effectively decrease the desorption energy consumption.^{19–21} However, solvents such as methanol, ethylene glycol (vapor pressure of 133 Pa, 20 °C), and propanediol (viscosity of 330 mPa·s, 40 °C) have shortcomings of high vapor pressure, toxicity, and high viscosity, which are not suitable for industrial operations. Therefore, the physical properties of solvents are crucial factors affecting their incorporation into industrial applications.

Poly(ethylene glycols) (PEGs), a kind of polar solvents, are frequently used as cosolvents in chemical and pharmaceutical processes. The end hydroxyl group forms hydrogen bonds between molecules, resulting in low saturated vapor pressure and high thermal stability. The highly polar hydroxyl group of PEGs can also interact with CO₂ molecules to promote the absorption.^{18,22} Li et al. previously utilized the PEGs as cosolvents to prepare the low concentrated amine/PEG200 and ionic liquid/PEGs absorbents, which exhibited excellent absorption and desorption performance.^{19,23,24} Among various PEG substances, the diethylene glycol and triethylene glycol are generally toxic, while PEG200 possesses excellent properties such as nontoxicity and no stimulation. In addition, the viscosity of PEGs increases with the molecular weights (e.g., 25.05 mPa·s for PEG200, 34.94 mPa·s for PEG300, and 44.4 mPa·s for PEG400 at 313 K). The increase of viscosity leads to the enhancement of mass-transfer resistance between a gas and liquid interface. Therefore, PEG200 is chosen as an auxiliary solvent when considering the nonaqueous amine solution.

Since these absorbents are developed for the industrial applications, in this paper, monoethanolamine (MEA) with relatively low viscosity (10.02 mPa·s at 313 K),²⁵ a fast CO₂ absorption rate, and low cost is selected to prepare the MEA/PEG200 absorbents. The CO₂ absorption rate and capacity, desorption rate and efficiency, cyclic stability, and the viscosity of the absorbent that varies with the absorption process are systematically investigated, and the performance of MEA/PEG200 is compared with that of MEA/H₂O. Finally, the isobaric specific heat capacity, reaction heat, and thermal stability of the 5 M MEA/PEG200 absorbent are also measured to evaluate the desorption energy consumption, as well as the corrosion behavior of absorbents on carbon steel.

2. EXPERIMENTAL SECTION

2.1. Materials. Poly(ethylene glycol) 200 (PEG200, AR) and monoethanolamine (MEA, 99%) were purchased from Chengdu Kelong Reagent co. Ltd. Nitrogen (99.99%) and carbon dioxide (99.99%) were purchased from Chengdu Qiaoyuan Gas Plant.

2.2. Apparatus and Procedures. **2.2.1. Absorption.** MEA/PEG200 and MEA/H₂O absorbents were prepared with the MEA molar concentrations of 0.5, 1, 2, 3, and 5 mol/L, respectively. As shown in Figure 1, 100 mL of the as-prepared solution was transferred into a three-necked flask (250 mL) and heated to 40 °C in a water bath with magnetic stirring at 300 rpm. A feeding stream of mixed gas (CO₂ volume fraction of 15%) was bubbled through the solution at a constant flow rate of 300 mL/min. The off gas of absorption was measured using an infrared CO₂ analyzer (FN316B, Shanxi Feiente Instrument Technology Co., Ltd.). The absorption experiment ceased after the CO₂ concentration of the off gas stabilized for 10 min. The CO₂ content absorbed in the solution was determined by titration analysis.²⁶

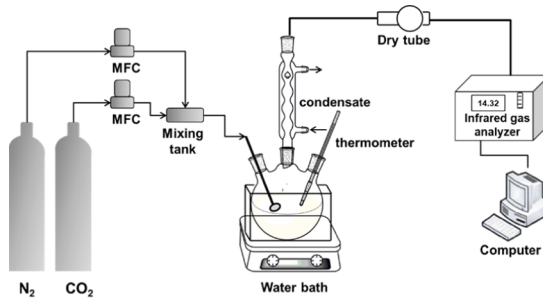


Figure 1. Schematic diagram of the CO₂ absorption and desorption device.

2.2.2. Desorption. A CO₂-rich solution with a CO₂/MEA molar ratio of 0.45–0.50 was desorbed in a three-necked flask, in which the CO₂-rich solution was heated to 80 °C under magnetic agitation at 300 rpm. N₂ was used as a purge gas at a flow rate of 200 mL/min. The off gas was detected until the CO₂ concentration stabilized at less than 1.0% for 10 min. The regenerated solution was also analyzed via titration analysis.

2.2.3. Corrosion Evaluation. C20 steel was selected as the probe material to evaluate the corrosion behavior of the absorbent system. The weight of each C20 sample was 1.40–1.50 g and the size was about 8.0 × 30.0 × 1.0 mm. The samples were immersed in the solutions (both the fresh and CO₂-rich MEA/PEG200 or MEA/H₂O) for 30, 120, and 400 days, respectively.

2.3. Calculation and Analysis Methods. **2.3.1. Absorption and Desorption Calculation.** The absorption and desorption rates of CO₂ were calculated by eqs 1 and 2, respectively. The CO₂ content of absorbed and desorbed solutions can be obtained by eqs 3 and 4, respectively. The volumetric CO₂ content in a liquid phase was also determined by titration and calculated by eq 5. The desorption ratio was defined as the ratio of CO₂ contents in the solutions before and after desorption (eq 6).

$$r_{\text{abs}} = \frac{V_{\text{SFG}}(y_{\text{CO}_2}^{\text{in}} - y_{\text{CO}_2}^{\text{out}})}{1 - y_{\text{CO}_2}^{\text{out}}} \times \frac{PM_{\text{CO}_2}}{RTV_{\text{sol}}} \quad (1)$$

$$r_{\text{des}} = \frac{V_{\text{N}_2}y_{\text{CO}_2}^{\text{out}}}{1 - y_{\text{CO}_2}^{\text{out}}} \times \frac{PM_{\text{CO}_2}}{RTV_{\text{sol}}} \quad (2)$$

$$\alpha_{\text{abs}} = \frac{\int_0^t r_{\text{abs}} dt}{M_{\text{CO}_2} \times V_{\text{sol}} \times C_{\text{MEA}}} \quad (3)$$

$$\alpha_{\text{des}} = \frac{\int_0^t r_{\text{des}} dt}{M_{\text{CO}_2} \times V_{\text{sol}} \times C_{\text{MEA}}} \quad (4)$$

$$V_{\text{L-CO}_2} = V_2 - V_1 - V'_{\text{HCl}} \quad (5)$$

$$\eta = \frac{\alpha_{\text{CO}_2\text{-rich}} - \alpha_{\text{CO}_2\text{-poor}}}{\alpha_{\text{CO}_2\text{-rich}}} \quad (6)$$

2.3.2. Estimation of CO₂ Desorption Energy Consumption. The CO₂ desorption is the major energy-consuming process in CO₂ capture.²⁷ The energy consumption of desorption can be calculated by eq 7, including sensible heat

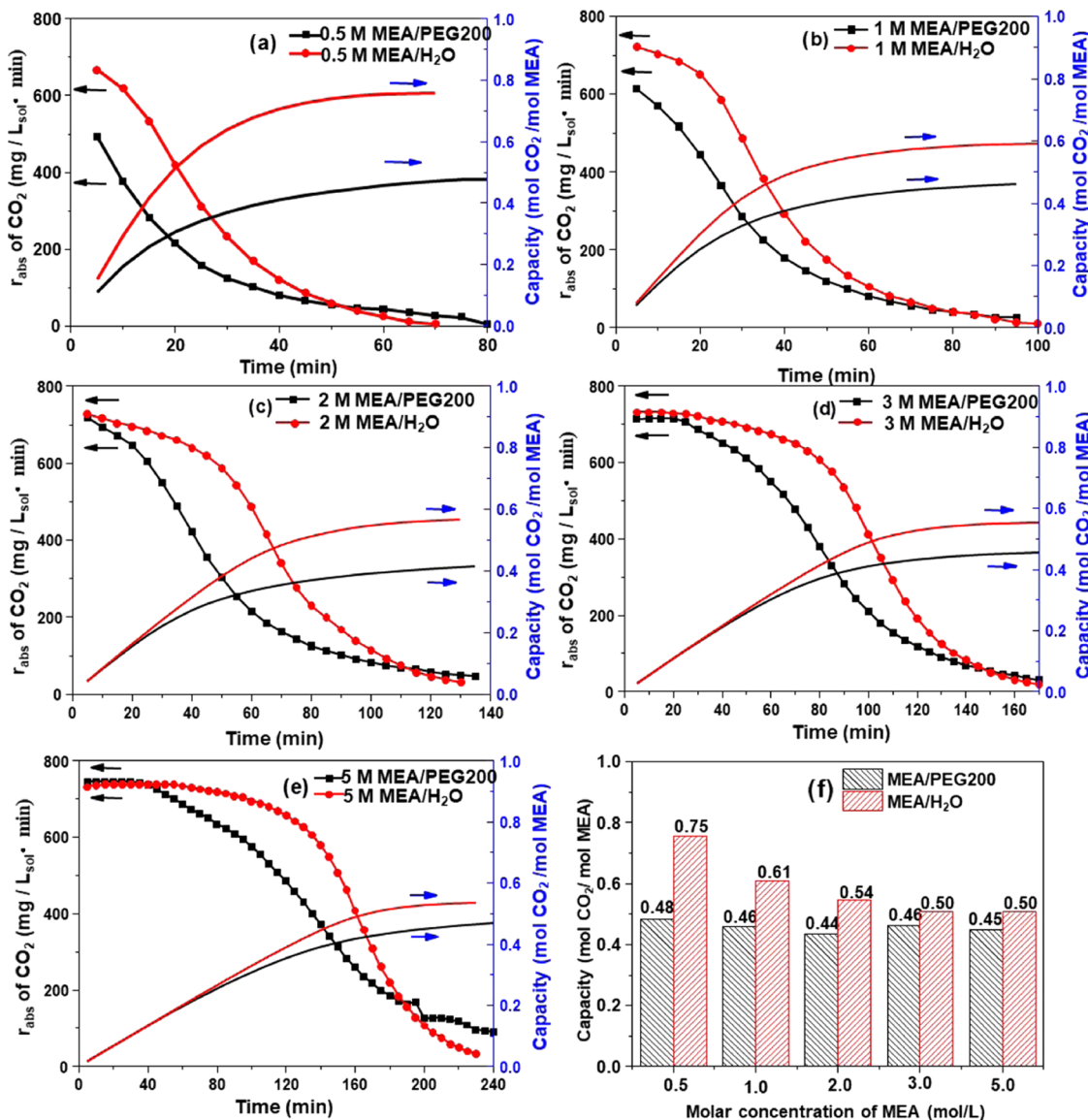


Figure 2. CO₂ absorption rates and capacity of the MEA/PEG200 and MEA/H₂O absorbents, respectively. (a) 0.5 M, (b) 1 M, (c) 2 M, (d) 3 M, (e) and 5 M. (f) CO₂ capacity of absorbents at different MEA concentrations determined by titration analysis.

of solution, reaction heat of the desorption process, and latent heat of solvent vaporization.

$$Q = H_{\text{sensible}} + H_{\text{reaction}} + H_{\text{vapor}} \quad (7)$$

For 1 kg of CO₂, the sensible heat of solution was calculated by eqs 8–10

$$H_{\text{sensible}} = m_{\text{solv}} C_p \Delta T \quad (8)$$

$$m_{\text{solv}} = \frac{1000}{M_{\text{CO}_2}} \times \eta \times \alpha_{\text{rich}} \times C_{\text{MEA}} \times \rho_{\text{solv}} \quad (9)$$

$$c_p = c_{\text{MEA}} \times \phi + c_{\text{solvent}} \times (1 - \phi) \quad (10)$$

According to the literature,²⁸ the reaction heat was calculated by eqs 11–13,

$$H_{\text{reaction}} = \frac{m_{\text{CO}_2}}{M_{\text{CO}_2}} \Delta H_{\text{abs}, \text{CO}_2} \quad (11)$$

$$q = \frac{(Y_2 - Y_1)}{44} \quad (12)$$

$$\Delta H_{\text{abs}, \text{CO}_2} = \frac{\Delta H_{\text{adsorbent}}}{q} \times 10^{-3} \quad (13)$$

The latent heat of evaporation, as shown in eq 14, the partial pressure ratio of the volatile solvent, and CO₂ can be calculated by the method proposed by Wang et al.²⁹

$$H_{\text{vapor}} = \Delta H_{\nu, \text{sol}} \times \frac{P_{\text{sol}}}{P_{\text{CO}_2}} \times \frac{1}{M_{\text{CO}_2}} \quad (14)$$

2.3.3. Analysis Method. 2.3.3.1. Determination of Reaction Heat and Thermal Capacity. Differential scanning from 20 to 92 °C was performed on a calorimeter (NETZSCH DSC214) to measure the isobaric specific heat capacity of the solvent at a heating rate of 2 °C/min under N₂ gas protection (20 mL/min).³⁰ As the gas stream containing CO₂ bubbled through the absorbents at 40 °C with a flow rate of 20 mL/min, a synchronous thermal analyzer (NETZSCH STA 449

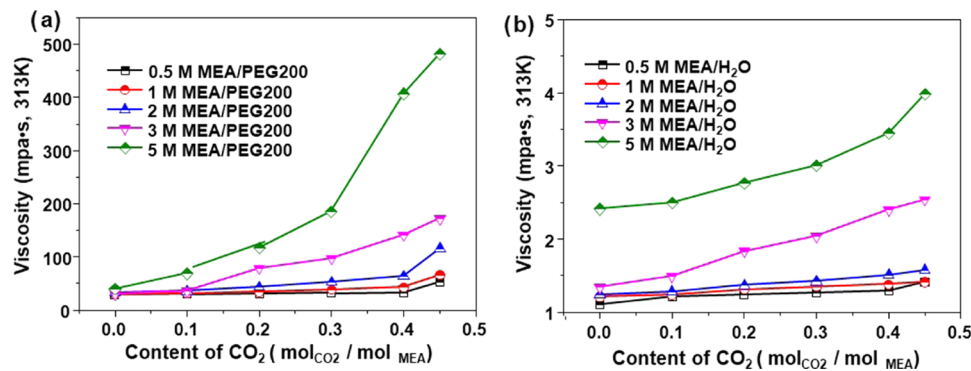


Figure 3. Viscosity changes of the MEA/PEG200 and MEA/H₂O solutions under different CO₂ and MEA concentrations at 313 K.

F3) was employed to measure the weight change and heat effect of absorbents during absorption. Therefore, the reaction heat and volatility could be estimated. Thermogravimetric (TG) analysis of the fresh and CO₂-rich absorbents was evaluated in 5 mL/min N₂ at 80 °C for 60 min.

2.3.3.2. Determination of Vapor Pressure. The vapor pressure of the absorbents was tested using an automatic vapor pressure tester (HY8017 Jilin Hong Yuan Scientific Instrument Co., Ltd.).

2.3.3.3. Viscosity Measurement. The CO₂-absorbed rich-phase solution and the original MEA/PEG200 solution were mixed to obtain the solutions with CO₂ content of 0.10–0.45 mol/mol MEA. The viscosity was measured using a rotating viscometer (Shanghai Changji Geological Instrument Co., Ltd.) under 40 °C.

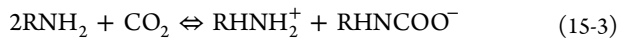
2.3.3.4. Inductively Coupled Plasma Optical Emission Spectrometer (ICP-OES) Analysis. The iron contents of these solutions were detected by an inductively coupled plasma emission spectrometer (ICP-OES) using an Arco's detector (Spectro).

2.3.3.5. Determination of the Polarization Curve. The corrosion current density of C20 steel in different solutions was tested by the electrochemical method. The polarization curve (Tafel curve) was determined using the electrochemical workstation (CHI 760E Shanghai Chenhua Instrument Co., Ltd.)

2.3.3.6. ¹³C NMR Analysis. ¹³C NMR spectra were obtained using a JNM ECZ400S/L1 spectrometer. To provide enough signals for the deuterium lock, deuterated dimethyl sulfoxide (DMSO-*d*₆) or D₂O was introduced into the NMR tube containing the fresh and CO₂-rich absorbents.

3. RESULTS AND DISCUSSION

3.1. CO₂ Absorption Rate and Capacity. According to the zwitterion mechanism, primary amine can react with CO₂ to form the zwitterions.^{31–33} Under nonaqueous conditions, the hydrogen ion transfer occurs between the zwitterion and the amine (MEA) to produce RHNH₂⁺ and RHNCOO[−], as indicated in eqs 15-1–15-3. When the nonaqueous solvent is employed, the stoichiometric coefficient of amine and CO₂ is 2:1 in the reaction.



When H₂O exists in the solution, RHNCOO[−] is hydrolyzed to form RNH₂. Therefore, from the reaction formulas eqs 16-1 and 16-2, the reaction stoichiometry in the aqueous solution is 1:1, that is, the maximum absorption amounts of 1 mol alkanolamine is 1 mol CO₂. Therefore, in principle, MEA/H₂O could absorb more CO₂ than MEA/PEG200.

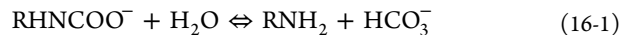


Figure 2a–e shows the CO₂ absorption rate and capacity of MEA/PEG200 and MEA/H₂O absorbents with the MEA concentration in the range of 0.5–5 M. When the MEA concentration was 0.5 and 1 M, the initial absorption rates (492 and 614 mg_{CO₂}/(L_{sol}·min)) in the MEA/PEG200 absorbents were lower than that of MEA/H₂O absorbents (667 and 722 mg_{CO₂}/(L_{sol}·min)), as shown in Figure 2a,b. Notably, when the MEA concentration exceeded 2 M (Figure 2c–e), the initial absorption rate of MEA/PEG200 absorbents was comparable to that of the MEA/H₂O absorbents (~720 mg_{CO₂}/(L_{sol}·min)). The increase in the MEA concentration may lead to the high MEA molecule density in the solution, which can shorten the CO₂ diffusion path and lower the diffusion resistance. Figure 2f reveals the CO₂ absorption capacity of absorbents with varying MEA concentrations. The CO₂ absorption capacity in the MEA/PEG200 absorbents with 0.5, 1, 2, 3, and 5 M are 0.48, 0.46, 0.44, 0.46, and 0.45 mol_{CO₂}/mol_{MEA}, respectively, which is close to the theoretical saturated capacity (0.50 mol_{CO₂}/mol_{MEA}). On the contrary, the saturated CO₂ absorption capacity in the MEA/H₂O absorbents decreases with the increase of the MEA concentration, and the actual capacity is about 50% of their theoretical capacity (1.0 mol_{CO₂}/mol_{MEA}) when the MEA concentration exceeds 3 M. The low capacity may be caused by the insufficient hydrolyzation of the RHNCOO[−] in aqueous solutions. With the increase of the MEA concentration, the ratio of hydrolyzed RHNCOO[−] becomes smaller, thus the corresponding saturated capacity of MEA/H₂O decreases.

In addition, the CO₂ absorption rate of MEA/PEG200 absorbents decreases rapidly compared with that of the MEA/H₂O absorbents. As shown in Figure 3, the viscosity of MEA/PEG200 absorbents exhibits an order of magnitude higher than that of the MEA/H₂O absorbents, which further increases significantly with the elevated CO₂ content. The viscosity of the 0.5 M MEA/PEG200 solution increased from 28.4 to 52.4 mPa·s, as the content of CO₂ in the solution increased from 0

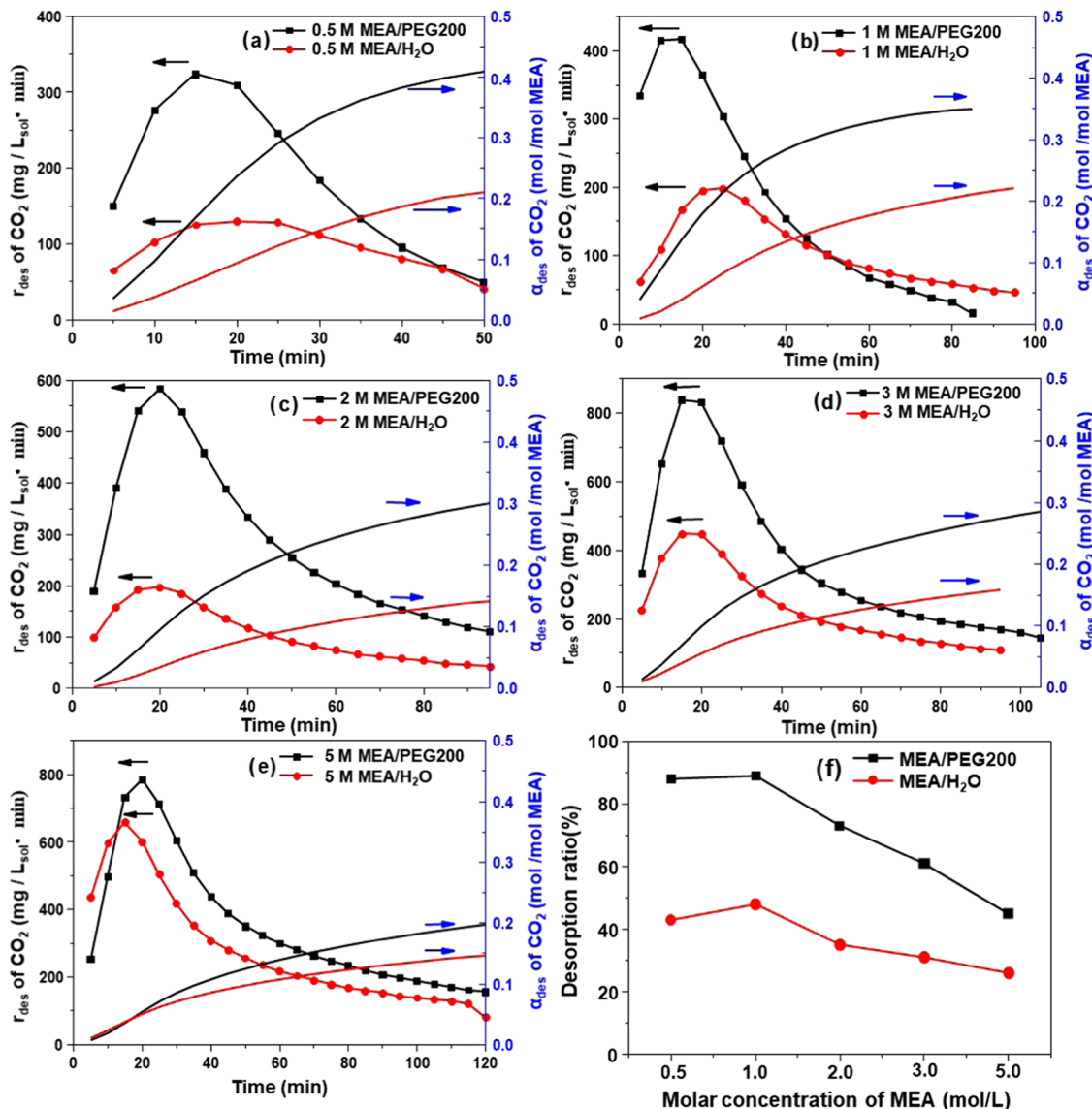


Figure 4. CO_2 desorption rate and the desorption ratio of the CO_2 -rich MEA/PEG200 and CO_2 -rich MEA/ H_2O , respectively. (a) 0.5 M; (b) 1 M; (c) 2 M; (d) 3 M; (e) 5 M; and the (f) desorption ratio of the CO_2 -rich absorbents at different MEA concentrations.

to 0.45 mol/mol_{MEA}. Moreover, under the same CO_2 content, the viscosity of the 5 M MEA/PEG200 solution increased from 40.2 to 481 mPa·s. In comparison, the viscosity of MEA/ H_2O solutions remains below 5.0 mPa·s in any condition. The high viscosity values result in high gas diffusion resistance, thereby reducing the CO_2 absorption rate.

3.2. CO_2 Desorption Rate and Efficiency. The CO_2 desorption rate and efficiency of the CO_2 -rich MEA/PEG200 and MEA/ H_2O absorbents are shown in Figure 4. The initial desorption reaction temperature (60°C) of the MEA/PEG200 absorbents is detected to be lower than that of the MEA/ H_2O (70°C). The maximum CO_2 desorption rate of MEA/PEG200 (0.5 M) is $323 \text{ mg}_{\text{CO}_2}/(\text{L}_{\text{sol}} \cdot \text{min})$, which is greater than that of the MEA/ H_2O ($129 \text{ mg}_{\text{CO}_2}/(\text{L}_{\text{sol}} \cdot \text{min})$). Notably, the desorption rates of absorbents with varying MEA concentrations reveal a volcanic-like trend along with the reaction time (Figure 4a–e). With the increase of the MEA concentration in a CO_2 -rich solution, the maximal CO_2 desorption rate increases; the highest maximal desorption rate of $838 \text{ mg}_{\text{CO}_2}/(\text{L}_{\text{sol}} \cdot \text{min})$ can be obtained for 3 M MEA/

PEG200. When the concentration further increases to 5 M, the maximal desorption rate exhibits a certain decrease ($782 \text{ mg}_{\text{CO}_2}/(\text{L}_{\text{sol}} \cdot \text{min})$), which may be due to the sluggish diffusion efficiency of the desorption generated CO_2 from the high-viscosity solution. However, the desorption rate is still higher than that of the CO_2 -rich MEA/ H_2O absorbents, which may be due to the much lower decomposition energy barrier of a nonaqueous solution than that of an aqueous solution.³⁴

The desorption efficiencies of the MEA/PEG200 and MEA/ H_2O absorbents are calculated by eq 6 and shown in Figure 4f. With the increase of the MEA concentration, the desorption efficiency of MEA/PEG200 decreases from 88.0% (0.5 M, 50 min) to 44.4% (5.0 M, 120 min), which is still higher than that of the corresponding MEA/ H_2O absorbents (decreased from 43.0% (0.5 M, 50 min) to 26.0% (5.0 M, 120 min)). The absorbents with a high MEA concentration generally possess high viscosity, which restricts the mass transfer between the CO_2 gas and liquid phases, thus resulting in the decreased desorption efficiency of the desorbed CO_2 gas in the viscous solution.

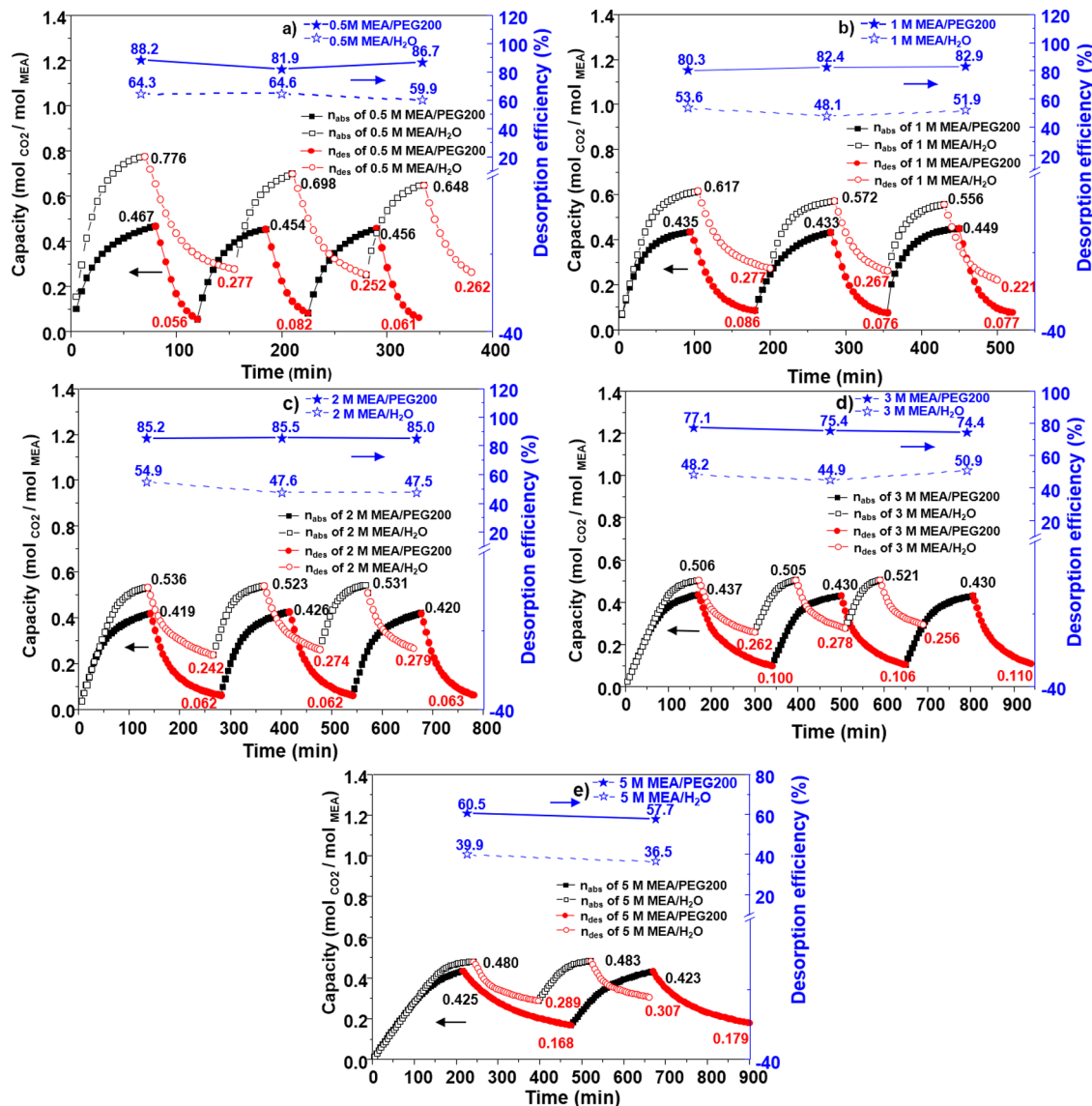


Figure 5. Cyclic absorption and desorption rates of the MEA/PEG200 and MEA/H₂O at different concentrations. (a) 0.5 M; (b) 1 M; (c) 2 M; (d) 3 M; and (e) 5 M.

3.3. Cyclic Absorption and Desorption Ability. To further evaluate the cyclic performance of the absorbents, the cyclic absorption and desorption efficiency of all absorbents are investigated. As shown in Figure 5a–d, the absorption capacities of the 0.5–3 M MEA/PEG200 absorbents are stable within three cycles, while the desorption efficiency presents a high level (about 85.0% for 0.5 to 2 M and 75.0% for 3 M), especially under the MEA concentration lower than 0.1 mol_{CO₂}/mol_{MEA}. Figure 5e reveals that the desorption efficiency of the 5 M MEA/PEG200 remains above 55.0% after passing through two cycles. By contrast, a high value of the CO₂ residue (0.25–0.30 mol_{CO₂}/mol_{MEA}) is detected in all of the MEA/H₂O absorbents after desorption, leading to a low cyclic desorption efficiency. Therefore, the MEA/PEG200 absorbents exhibit high cyclic stability and high CO₂ absorption/desorption efficiency, and the results are also shown in Table S1.

3.4. Absorbent Thermal Stability. The thermal stability of the absorbent is also crucial for a continuous CO₂ absorption and desorption process since the desorption

temperature is about 80 °C and the evaporation latent heat greatly affects the energy consumption. Figure 6 exhibits the TG curves of the fresh and CO₂-rich absorbents in a N₂ atmosphere at 80 °C for 60 min. The results indicate a weight loss of 10.19% for the fresh 5 M MEA/PEG200 absorbent and

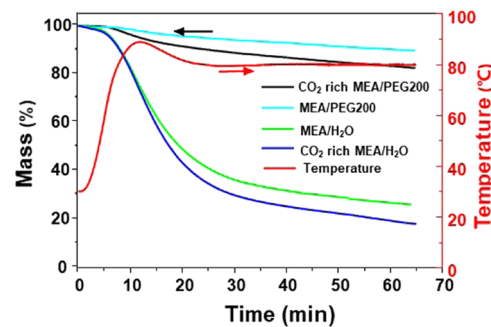


Figure 6. Thermogravimetric analysis curves of the fresh and CO₂-rich absorbents (5 M MEA/PEG200 and 5 M MEA/H₂O).

19.98% for the CO₂-rich one, attributing to the partial CO₂ desorption. However, a significant weight loss is observed with a value of 73.98 and 81.87% for the fresh and CO₂-rich 5 M MEA/H₂O absorbents, respectively. As shown in Table 1, the

Table 1. Saturated Vapor Pressure of Different Solutions

	T (°C)	P ^s (Pa)
MEA	80	2237 ³⁵
H ₂ O	80	47370
PEG200	85	9.9 ³⁶
5 M MEA/PEG200	80	1800
5 M MEA/H ₂ O	80	26 700

saturated vapor pressure of the MEA is 2237 Pa (80 °C).³⁵ Additionally, the saturated vapor pressure of PEG200 is only 9.9 Pa (95 °C),³⁶ which is much lower than that of water (47 370 Pa, 80 °C). Thus, when PEG200 is used as the cosolvent, the saturated vapor pressure of the 5 M MEA/PEG200 solution (1800 Pa, 80 °C) is much lower than that of the 5 M MEA/H₂O solution (26 700 Pa, 80 °C). The low volatility of the MEA/PEG200 absorbent can significantly decrease the mass loss ratio of the absorbent and effectively reduce the latent heat during the carbon capture process.

3.5. Estimation of the Desorption Energy Consumption. To obtain the energy consumption in the regeneration process, the energy consumption of the CO₂-rich MEA/PEG200 and MEA/H₂O absorbents is evaluated during the desorption process using 1 kg of CO₂ as the basis (Figure S1). The energy consumption during the desorption is mainly composed of the sensible heat of solution, reaction heat of the desorption process, and latent heat of vaporization.²⁷

3.5.1. Sensible Heat of the Solution. The cyclic stability test results (Figure 5e) are used to evaluate the sensible heat during the desorption process. The average isobaric specific heat capacity (C_p) of the PEG200 solution detected by differential scanning calorimetry (DSC) at 30–90 °C is 2.37 kJ/(kg·K) (Figure S2), which is consistent with the reported value (C_p = 2.13 kJ/(kg·K) at 60 °C).²¹ In addition, the C_p, MEA value of 3.36 kJ/(kg·K) can also be observed. According to the eqs 8–10, the calculated sensible heat values (Table 2) of MEA/PEG200 and MEA/H₂O absorbents are 1052 and 1961 kJ/kg_{CO₂}, respectively.

Table 2. Desorption Energy Consumption of the Two Absorbents (kJ/kg_{CO₂})

	MEA/H ₂ O	MEA/PEG200
MEA concentration	5 M	5 M
sensible heat	1961.00	1052.00
reaction enthalpy	1795.00 ³⁸	1495.00
latent heat of vaporization	65.59	0.00
total energy consumption for regeneration	3821.59	2547.00

3.5.2. Reaction Heat during the Desorption Process. The desorption reaction heat in the CO₂-rich 5 M MEA/PEG200 absorbent is measured by TG and DSC. The calculated reaction heat is 65.8 kJ/mol for the CO₂ desorption reaction in the CO₂-loaded (0.4 mol_{CO₂}/mol_{MEA}) MEA/PEG200 absorbent (Figure S3), while that of the MEA/H₂O absorbent is 79–84 kJ/mol.^{22,23} The reaction heat values are also listed in Table 2, that is, 1495 kJ/kg_{CO₂} for MEA/PEG200 absorbents and

1795 kJ/kg_{CO₂} for MEA/H₂O. This slight difference lies in the different reaction intermediates (Section 3.6 in detail).

3.5.3. Latent Heat during the Desorption Process. The vaporization latent heat of the solution during desorption is the phase-change heat. As the desorption temperature (80 °C) is lower than the vaporization temperature of each component in the solution, the sensible heat is the main energy input in the process. However, some absorbent solutions can also be removed during the continuous escape of the CO₂ gas flow. As shown in eq 14, the vaporization latent heat of the solution is mainly determined by partial pressures of the outlet CO₂ and the solution. Since the 5 M MEA/PEG200 absorbent with a high boiling point and low volatility exhibits excellent thermal stability (Table 1 and Figure 6), the latent heat of the solution vaporization can be ignored. On the contrary, according to the calculation method proposed by Wang et al.,²⁹ the latent heat of vaporization of 5 M MEA/H₂O is 65.59 kJ/kg_{CO₂} at the temperature of 80 °C. The previous work has reported that the capture of 1 kg of CO₂ would produce 0.03 kg of steam,²¹ which is in line with the results in this work.

As summarized in Table 2, the estimated energy consumption for CO₂ regeneration in the 5 M MEA/PEG200 solution is 2.547 MJ/kg_{CO₂}, which is 33% lower than that of the MEA/H₂O (3.821 MJ/kg_{CO₂}). Moreover, the loss of organic amines during the desorption process can also be reduced when utilizing PEG200 as a cosolvent.

3.6. Corrosion Evaluation of Carbon Steel. The corrosion of the absorbents on the C20 steel is an important parameter to determine the equipment safety and operation cost of the process. The corrosion behaviors of the fresh and CO₂-rich absorbents are tested by immersing the carbon steel plates in the solutions for 30, 120, and 400 days, respectively. As shown in Figure S4, the MEA/PEG200 absorbents exhibit a slightly corrosive effect on the steel, and the solution remains clear after immersion for 400 days (Figure 7a). On the contrary, the steel samples in the MEA/H₂O absorbents are seriously corroded and the solution is obviously dyed. The polarization curves of C20 steel in different solutions are also shown in Figure 7b. The relationship between the current density of the solutions is MEA/PEG200 < CO₂-rich MEA/PEG200 < MEA/H₂O < CO₂-rich MEA/H₂O, which corresponds to the conductivity value of the solutions (Figure 7a). According to Faraday's law, there is a strict correspondence between the metal corrosion rate and self-corrosion current. As shown in Figure 7a, ICP results also confirmed the slight corrosion on carbon steel in the MEA/PEG200 solutions. The concentrations of the Fe ions are only 25.2 and 12.6 mg/L in the MEA/PEG200 and CO₂-rich MEA/PEG200 solutions after 30 days, respectively, while that in MEA/H₂O and CO₂-rich MEA/H₂O are 31.8 and 483.0 mg/L, respectively. By prolonging the immersion period, only a tiny increment of Fe ions is detected in the fresh (32.0 mg/L) and CO₂-rich (45.0 mg/L) MEA/PEG200 solutions, respectively, indicating the excellent anticorrosion ability of the MEA/PEG200 solution. However, in MEA containing aqueous solutions, the concentrations of Fe ions of fresh and CO₂-rich MEA/H₂O are 714.0 and 2114.0 mg/L, respectively. These high values also suggest the serious corrosion of the steel. Moreover, the weight values of the C20 steel before and after immersing for different times are shown in Table S2, and the results are in line with the ICP results. The corrosion experiments further reveal that the MEA/PEG200 absorbent

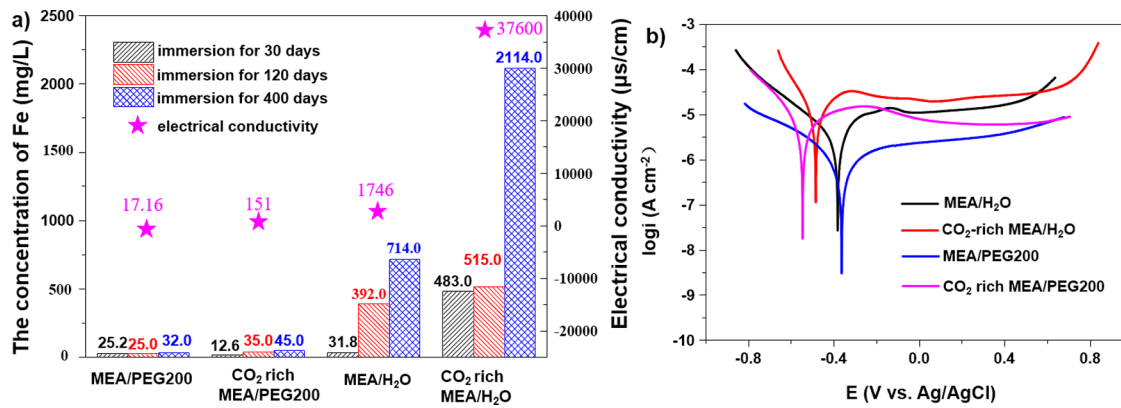


Figure 7. (a) ICP results of the Fe concentration after various C20 steel immersion times in various solutions. (a) Electrical conductivity and (b) polarization curves of the various solutions.

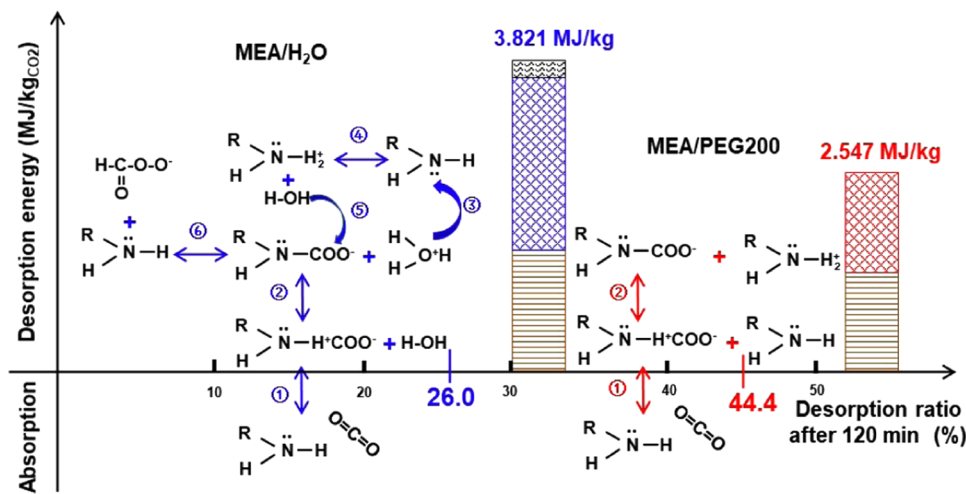


Figure 8. Summary of the reaction mechanism, desorption ratio after 120 min, and total regeneration energy consumption of CO₂ captured by 5 M MEA/PEG200 and 5 M MEA/H₂O.

may lower the cost of anticorrosion materials required from the equipment for industrial CO₂ capture.

3.7. Reaction Mechanism in MEA/PEG200 and MEA/H₂O Absorbents. To further confirm the difference in the reaction mechanism between the CO₂ trapping process in the aqueous and nonaqueous absorbents, the qualitative analysis of the NMR is performed. As shown in Figures S5 and S6, only RHNCOO⁻ is generated during the CO₂ capture process using the MEA/PEG200 absorbent. However, the products of the CO₂-rich MEA/H₂O absorbent are more complicated, including RHNCOO⁻ and HCO₃⁻/CO₃²⁻, which is consistent with the refs 20 and 37 and eqs 15-1–15-3 and 16-1–16-2. To summarize the typical difference between the MEA/PEG200 and MEA/H₂O absorbents, the reaction routes, the desorption ratio after 120 min, and total energy consumption are proposed in Figure 8. First, the aqueous and nonaqueous absorbents exhibit different reaction routes, and more complicated products are produced in the aqueous absorbent in the presence of H₂O. Second, the desorption ratio after 120 min of the MEA/PEG200 absorbent is obviously higher than that of the MEA/H₂O system (44.4 and 26.0%, respectively), which may be due to the much lower decomposition energy barrier of a nonaqueous solution.³⁴ Finally, the total desorption energy consumption of the MEA/PEG200 absorbent (2.547 MJ/kg) is lower than that of the MEA/H₂O system (3.821 MJ/kg).

MJ/kg), which is mainly due to the different sensible heat values of the aqueous and nonaqueous absorbents.

4. CONCLUSIONS

A nonaqueous MEA/PEG200 absorbent is successfully developed for CO₂ capture using an organic solvent. The absorption rate and capacity, desorption rate and efficiency, and cyclic stability of the absorbents are systematically investigated in the MEA/PEG200 sorbent and the results are compared with that of the MEA/H₂O absorbent. The MEA/PEG200 absorbent with the MEA concentration above 3 mol/L exhibits the highest desorption rate (838 mg_{CO₂}/(L_{sol}·min)) and excellent cyclic stability (deviation < 4%), which is much superior to the MEA/H₂O absorbent (the desorption rate of 447 mg_{CO₂}/(L_{sol}·min)). In addition, the energy consumption for CO₂ regeneration in the 5 M MEA/PEG200 solution is 33% lower than that in the MEA/H₂O solution. Moreover, low corrosion on carbon steel is found during 400-day immersion with a weight loss of 0.65 and 0.68% for fresh and CO₂-rich MEA/PEG200 solutions, respectively. Therefore, this low-energy-consuming and anticorrosion MEA/PEG200 absorbent possesses enormous potential for CO₂ capture in the industry.

■ ASSOCIATED CONTENT

SI Supporting Information

The Supporting Information is available free of charge at <https://pubs.acs.org/doi/10.1021/acs.iecr.0c05294>.

The flow chart of the CO₂ capture process, the DSC curve, the TG-DSC diagram, the optical images, ¹³C NMR spectra, cyclic performance, and the corrosion rate (PDF)

■ AUTHOR INFORMATION

Corresponding Author

Bin Liang – Low-Carbon Technology and Chemical Reaction Engineering Laboratory, School of Chemical Engineering and Institute of New Energy and Low-Carbon Technology, Sichuan University, Chengdu 610065, China; orcid.org/0000-0003-2942-4686; Phone: (+86) 28-85990278; Email: liangbin@scu.edu.cn

Authors

Wen Tian – Low-Carbon Technology and Chemical Reaction Engineering Laboratory, School of Chemical Engineering, Sichuan University, Chengdu 610065, China

Kui Ma – Low-Carbon Technology and Chemical Reaction Engineering Laboratory, School of Chemical Engineering, Sichuan University, Chengdu 610065, China; orcid.org/0000-0002-5667-4755

Junyi Ji – Low-Carbon Technology and Chemical Reaction Engineering Laboratory, School of Chemical Engineering, Sichuan University, Chengdu 610065, China; orcid.org/0000-0002-5545-1357

Siyang Tang – Low-Carbon Technology and Chemical Reaction Engineering Laboratory, School of Chemical Engineering, Sichuan University, Chengdu 610065, China; orcid.org/0000-0003-4757-3992

Shan Zhong – Low-Carbon Technology and Chemical Reaction Engineering Laboratory, School of Chemical Engineering, Sichuan University, Chengdu 610065, China; orcid.org/0000-0002-0247-6788

Changjun Liu – Low-Carbon Technology and Chemical Reaction Engineering Laboratory, School of Chemical Engineering and Institute of New Energy and Low-Carbon Technology, Sichuan University, Chengdu 610065, China; orcid.org/0000-0003-3735-4112

Hairong Yue – Low-Carbon Technology and Chemical Reaction Engineering Laboratory, School of Chemical Engineering and Institute of New Energy and Low-Carbon Technology, Sichuan University, Chengdu 610065, China; orcid.org/0000-0002-9558-0516

Complete contact information is available at:

<https://pubs.acs.org/doi/10.1021/acs.iecr.0c05294>

Notes

The authors declare no competing financial interest.

■ ACKNOWLEDGMENTS

The authors are grateful for the support from the National Key R&D Program of China (Grant No. 2018YFB0605700) and the National Natural Science Foundation of China (22008157). We also appreciate Dr. Yanping Huang from Center of Engineering Experimental Teaching for the NMR measurement and analysis.

■ NOMENCLATURE

r_{abs}	absorption rate of CO ₂ (mg _{CO₂} /(L _{sol} ·min))
r_{des}	desorption rate of CO ₂ (mg _{CO₂} /(L _{sol} ·min))
V_{SFG}	inlet gas flow (mL/min)
$y_{\text{CO}_2}^{\text{in}}$	molar concentration of CO ₂ imported
$y_{\text{CO}_2}^{\text{out}}$	molar concentration of CO ₂ exported
V_{N_2}	N ₂ flow (mL/min)
α_{abs}	absorption of CO ₂ (mol/mol _{MEA})
α_{des}	desorption volume of CO ₂ (mol/mol _{MEA})
$V_{\text{L-CO}_2}$	content of CO ₂ in the liquid phase (mL)
η	desorption efficiency of CO ₂
H_{sensible}	sensible heat of solution (kJ/kg)
m_{solv}	solution quality (kg)
α_{rich}	capacity of CO ₂ in the rich liquid (mol _{CO₂} /mol _{MEA})
C_{solv}	molar content of MEA in the solution (mol/L)
ρ_{solv}	density of the mixed solution (kg/L)
M_{CO_2}	molecular weight of CO ₂
c_p	specific heat of the solution (kJ/kg·K)
φ	the mass fraction of MEA
H_{reaction}	heat of the reaction (kJ/kg)
q	the molar amount of CO ₂ per gram of the absorbent (mol _{CO₂} /g)
$\Delta H_{\text{abs,CO}_2}$	heat of the reaction per mole of CO ₂ (kJ/mol)
P_{CO_2}	CO ₂ partial pressure (Pa)
T	temperature (K)

■ REFERENCES

- (1) Energy Industry Review. Global Energy & CO₂ Status Report 2019. In *The Latest Trends in Energy and Emissions in 2019*; IEA, 2019.
- (2) Matter, J. M.; Stute, M.; Snaebjornsdottir, S. O.; Oelkers, E. H.; Gislason, S. R.; Aradottir, E. S.; Sigfusson, B.; Gunnarsson, I.; Sigurdardottir, H.; Gunnlaugsson, E.; Axelsson, G.; Alfredsson, H. A.; Wolff-Boenisch, D.; Mesfin, K.; Taya, D. F. D. I. R.; Hall, J.; Dideriksen, K.; Broecker, W. S. Rapid carbon mineralization for permanent disposal of anthropogenic carbon dioxide emissions. *Science* **2016**, *352*, 1312–1314.
- (3) Wang, W.; Liu, X.; Wang, P.; Zheng, Y.; Wang, M. Enhancement of CO₂ Mineralization in Ca²⁺-Mg²⁺-Rich Aqueous Solutions Using Insoluble Amine. *Ind. Eng. Chem. Res.* **2013**, *52*, 8028–8033.
- (4) Shangguan, W.; Song, J.; Yue, H.; Tang, S.; Liu, C.; Li, C.; Liang, B.; Xie, H. An efficient milling-assisted technology for K-feldspar processing, industrial waste treatment and CO₂ mineralization. *Chem. Eng. J.* **2016**, *292*, 255–263.
- (5) Feng, B.; Du, M.; Dennis, T. J.; Anthony, K.; Perumal, M. J. Reduction of Energy Requirement of CO₂ Desorption by Adding Acid into CO₂-Loaded Solvent. *Energy Fuels* **2010**, *24*, 213–219.
- (6) Idem, R.; Wilson, M.; Tontiwachwuthikul, P.; Chakma, A.; Veawab, A.; Aroonwilas, A.; Gelowitz, D. Pilot Plant Studies of the CO₂ Capture Performance of Aqueous MEA and Mixed MEA/MDEA Solvents at the University of Regina CO₂ Capture Technology Development Plant and the Boundary Dam CO₂ Capture Demonstration Plant. *Ind. Eng. Chem. Res.* **2006**, *45*, 2414–2420.
- (7) Chen, S. J.; Zhu, M.; Fu, Y.; Huang, Y. X.; Tao, Z. C.; Li, W. L. Using 13X, LiX, and LiPdAgX zeolites for CO₂ capture from post-combustion flue gas. *Appl. Energy* **2017**, *191*, 87–98.
- (8) Yue, H.; Zhao, Y.; Zhao, L.; Lv, J.; Wang, S.; Gong, J.; Ma, X. Hydrogenation of dimethyl oxalate to ethylene glycol on a Cu/SiO₂/cordierite monolithic catalyst: Enhanced internal mass transfer and stability. *AIChE J.* **2012**, *58*, 2798–2809.
- (9) Kittel, J.; Gonzalez, S. Corrosion in CO₂ Post-Combustion Capture with Alkanolamines - A Review. *Oil Gas Sci. Technol.* **2014**, *69*, 915–929.
- (10) Kittel, J.; Fleury, E.; Vuillemin, B.; Gonzalez, S.; Ropital, F.; Oltra, R. Corrosion in alkanolamine used for acid gas removal: From

- natural gas processing to CO₂ capture. *Mater. Corros.* **2012**, *63*, 223–230.
- (11) Hasib-ur-Rahman, M.; Siaj, M.; Larachi, F. Ionic liquids for CO₂ capture—Development and progress. *Chem. Eng. Process.* **2010**, *49*, 313–322.
- (12) Zhang, X.; Zhang, X.; Dong, H.; Zhao, Z.; Zhang, S.; Huang, Y. Carbon capture with ionic liquids: overview and progress. *Energy Environ. Sci.* **2012**, *5*, 6668–6681.
- (13) Zhu, K.; Lu, H.; Liu, C.; Wu, K.; Jiang, W.; Cheng, J.; Tang, S.; Yue, H.; Liu, Y.; Liang, B. Investigation on the Phase-Change Absorbent System MEA plus Solvent A (SA) + H₂O Used for the CO₂ Capture from Flue Gas. *Ind. Eng. Chem. Res.* **2019**, *58*, 3811–3821.
- (14) Zhang, S.; Shen, Y.; Wang, L.; Chen, J.; Lu, Y. Phase change solvents for post-combustion CO₂ capture: Principle, advances, and challenges. *Appl. Energy* **2019**, *239*, 876–897.
- (15) Machida, H.; Ando, R.; Esaki, T.; Yamaguchi, T.; Horizoe, H.; Kishimoto, A.; Akiyama, K.; Nishimura, M. Low temperature swing process for CO₂ absorption-desorption using phase separation CO₂ capture solvent. *Int. J. Greenhouse Gas Control* **2018**, *75*, 1–7.
- (16) Shamiri, A.; Shafeeyan, M. S.; Tee, H. C.; Leo, C. Y.; Aroua, M. K.; Aghamohammadi, N. Absorption of CO₂ into aqueous mixtures of glycerol and monoethanolamine. *J. Nat. Gas Sci. Eng.* **2016**, *35*, 605–613.
- (17) Kang, M.-K.; Cho, J.-H.; Lee, J.-H.; Lee, S.-S.; Oh, K.-J. Kinetic Reaction Characteristics of Quasi-Aqueous and Nonaqueous Sorbents for CO₂ Absorption Using MEA/H₂O/Ethylene Glycol. *Energy Fuels* **2017**, *31*, 8383–8391.
- (18) Aschenbrenner, O.; Styring, P. Comparative study of solvent properties for carbon dioxide absorption. *Energy Environ. Sci.* **2010**, *3*, 1106–1113.
- (19) Li, J.; You, C.; Chen, L.; Ye, Y.; Qi, Z.; Sundmacher, K. Dynamics of CO₂ Absorption and Desorption Processes in Alkanolamine with Cosolvent Poly(ethylene glycol). *Ind. Eng. Chem. Res.* **2012**, *51*, 12081–12088.
- (20) Guo, H.; Li, C.; Shi, X.; Li, H.; Shen, S. Nonaqueous amine-based absorbents for energy efficient CO₂ capture. *Appl. Energy* **2019**, *239*, 725–734.
- (21) Guo, H.; Li, H.; Shen, S. CO₂ Capture by Water-Lean Amino Acid Salts: Absorption Performance and Mechanism. *Energy Fuels* **2018**, *32*, 6943–6954.
- (22) Wiesmet, V.; Weidner, E.; Behme, S.; Sadowski, G.; Arlt, W. Measurement and modelling of high-pressure phase equilibria in the systems polyethyleneglycol (PEG)—propane, PEG—nitrogen and PEG—carbon dioxide. *J. Supercrit. Fluids* **2000**, *17*, 1–12.
- (23) Li, J.; Dai, Z.; Usman, M.; Qi, Z.; Deng, L. CO₂/H₂ separation by amino-acid ionic liquids with poly(ethylene glycol) as co-solvent. *Int. J. Greenhouse Gas Control* **2016**, *45*, 207–215.
- (24) Li, J.; Chen, L.; Ye, Y.; Qi, Z. Solubility of CO₂ in the Mixed Solvent System of Alkanolamines and Poly(ethylene glycol) 200. *J. Chem. Eng. Data* **2014**, *59*, 1781–1787.
- (25) Song, J. H.; Park, S. B.; Yoon, J. H.; Lee, H. Densities and viscosities of monoethanolamine plus ethylene glycol plus water. *J. Chem. Eng. Data* **1996**, *41*, 1152–1154.
- (26) Liang, Z.; Idem, R.; Tontiwachwuthikul, P.; Yu, F.; Liu, H.; Rongwong, W. Experimental study on the solvent regeneration of a CO₂-loaded MEA solution using single and hybrid solid acid catalysts. *AIChE J.* **2016**, *62*, 753–765.
- (27) Oexmann, J.; Kather, A. Minimising the regeneration heat duty of post-combustion CO₂ capture by wet chemical absorption: The misguided focus on low heat of absorption solvents. *Int. J. Greenhouse Gas Control* **2010**, *4*, 36–43.
- (28) Liu, Z. S.; Peng, Y. H.; Huang, C. Y.; Hung, M. J. Application of thermogravimetry and differential scanning calorimetry for the evaluation of CO₂ adsorption on chemically modified adsorbents. *Thermochim. Acta* **2015**, *602*, 8–14.
- (29) Wang, J.; Sun, T.; Zhao, J.; Deng, S.; Li, K.; Xu, Y.; Fu, J. Thermodynamic considerations on MEA absorption: Whether thermodynamic cycle could be used as a tool for energy efficiency analysis. *Energy* **2019**, *168*, 380–392.
- (30) Piekarski, H.; Tkaczyk, M.; Tyczyńska, M. Heat capacity and phase behavior of aqueous diethylene glycol n-pentyl ether by DSC. *Thermochim. Acta* **2012**, *550*, 19–26.
- (31) Jing, G.; Zhou, L.; Zhou, Z. Characterization and kinetics of carbon dioxide absorption into aqueous tetramethylammonium glycinate solution. *Chem. Eng. J.* **2012**, *181–182*, 85–92.
- (32) Caplow, M. Kinetics of Carbamate Formation and Breakdown. *J. Am. Chem. Soc.* **1968**, *67*, 6795–6803.
- (33) Blauwhoff, P. M. M.; Versteeg, G. F.; Swaaij, W. P. M. V. A Study on the Reaction Between CO₂ and Alkanolamines in Aqueous Solutions. *Chem. Eng. Sci.* **1984**, *39*, 207–225.
- (34) Zhang, T. T.; Yu, Y. S.; Zhang, Z. X. Effects of non-aqueous solvents on CO₂ absorption in monoethanolamine: Ab initio calculations. *Mol. Simul.* **2018**, *44*, 815–825.
- (35) Avlund, A. S.; Kontogeorgis, G. M.; Michelsen, M. L. Modeling systems containing alkanolamines with the CPA equation of state. *Ind. Eng. Chem. Res.* **2008**, *47*, 7441–7446.
- (36) Aschenbrenner, O.; Supasitmongkol, S.; Taylor, M.; Styring, P. Measurement of vapour pressures of ionic liquids and other low vapour pressure solvents. *Green Chem.* **2009**, *11*, 1217–1221.
- (37) Ciftja, A. F.; Hartono, A.; Svendsen, H. F. C-13 NMR as a method species determination in CO₂ absorbent systems. *Int. J. Greenhouse Gas Control* **2013**, *16*, 224–232.
- (38) Song, H.-J.; Lee, S.; Park, K.; Lee, J.; Chand Spah, D.; Park, J.-W.; Filburn, T. P. Simplified Estimation of Regeneration Energy of 30 wt % Sodium Glycinate Solution for Carbon Dioxide Absorption. *Ind. Eng. Chem. Res.* **2008**, *47*, 9925–9930.